LAMINAR CONVECTIVE HEAT TRANSFER OF NANOFLUIDS IN A MICROCHANNEL HEAT SINK WITH INTERNAL LONGITUDINAL FINS.

J.H. SÁNCHEZ and J.C. ORTIZ

Department of Chemical Engineering, Universidad Pontificia Bolivariana, Medellín, Colombia.
E-mail: jorgeh.sanchez@upb.edu.co

***Abstract*— The conjugate heat transfer and fluid flow of three different water-based nanofluids (Al_2O_3, CuO, ZnO) through a finned square microchannel heat sink (MCHS) was studied numerically. Three-dimensional numerical simulations were performed considering both laminar flow and viscous dissipation effect along the microchannel. A constant heat flux was assumed on the external surface of the microchannel. The MCHS performance is evaluated in terms of the heat transfer coefficient, pressure drop, and thermal resistance for constant inlet velocity. The results show an increase in the heat transfer and pressure drop for nanofluids, while the thermal resistance of the microchannel decreases. A slight increase for developed Nusselt number is achieved for the finned MCHS in comparison with an unfinned channel.**

***Keywords*— Microchannel, Internal fins, Nanofluids, Convective heat transfer.**

I. INTRODUCTION

Microscale heat transfer is an important aspect in the design of components for the microelectronics industry due to the requirement of heat removal of electronic devices (Sobhan and Peterson, 2008; Ijam and Saidur, 2012). The analysis of heat transfer processes during the operation of such components represents an interesting avenue to improve thermal systems in those devices (Mohammed *et al.*, 2011). Because the heat transfer rate mainly depends on the surface area to volume ratio and properties of the cooling fluid, reduction on channel dimensions, coupling of fins, and a cooling fluid with an increased thermal conductivity, may contribute to enhanced thermal dissipation. The idea of size reduction was first implemented by Tuckerman and Peace (1981) by building a microchannel heat sink for high heat flux removal from silicon substrates. They observed heat dissipation was of about 790 W/cm^2, with temperature rise of 71ºC above the inlet temperature for the cooling fluid. On the other hand, improving the heat transfer properties of the cooling fluid can yield higher heat transfer coefficients. Hence, the suspension of nanoparticles with average sizes below 100 nm in conventional heat transfer fluids such as water, oil, or ethylene glycol, have shown to increases the effective thermal conductivity and heat transfer coefficient of the base fluid (Das *et al.*, 2008; Kakac and Pramuanjaroenkij, 2009; Godson *et al.*, 2010). These suspensions are conventionally referred as Nanofluids, a term first coined by Choi and Eastman (1995). Thus, nanofluids have been successfully incorporated in microchannels to improve heat transfer dissipation in a variety of electronic devices (Lee and Garimella, 2006; Jung *et al.*, 2009; Mohammed *et al.*, 2011).

The anomalous high thermal conductivity of nanofluids have been explained in light of several mechanistic descriptions including (Keblinski *et al.*, 2002; Das *et al.*, 2008; Kakac and Pramuanjaroenkij, 2009; Godson *et al.*, 2010), (1) transfer of energy due to collisions between particles during translational Brownian motion, (2) the existence of lower thermal resistance paths by particles clustering, (3) thermophoresis, (4) convection-like effects at the nanoscale due to the Brownian movement of the particles, among others. Bhattacharya *et al.* (2004) accurately predicted the thermal conductivity of nanofluids via Brownian dynamics simulations. Jang and Choi (2004) derived a model for thermal conductivity of nanofluids based on three different modes of energy transport: kinetics, thermal diffusion, and convection, which agrees with experimental results for different nanofluids. On the other hand, through an order-of-magnitude analysis, Prasher *et al.* (2005, 2006) showed that convection caused by Brownian translational movement of the particles appears to be the main mechanism responsible for the enhancement of the thermal conductivity of nanofluids.

The convective heat transfer of nanofluids in microchannels has attracted considerable attention in the last few years. Most of these studies coincide that the heat transfer coefficient is substantially increased in the nanofluid (Kakac and Pramuanjaroenkij, 2009). According to Chein and Huang (2005) and Chein and Chuang (2007), Cu-H_2O and CuO-H_2O nanofluids enhance the performance of a MCHS when compared with water as cooling fluid. Similar results were found numerically by Jang and Choi (2006), who showed that water-based nanofluids containing diamond particles increase the cooling performance and reduce the thermal resistance of a microchannel compared with the use of water as substrate. Jung *et al.* (2009) measured the heat transfer coefficient of Al_2O_3 nanofluids in microchannels. It was found that the Nusselt number increases with increasing the Reynolds number in laminar flow regime. Also, this study reported on a correlation for the Nusselt number under laminar flow in terms of the volume fraction of nanoparticles (non-homogeneous model), which agrees

with Heris *et al.* (2006) results about homogeneous models are not able to predict heat transfer coefficient enhancement of nanofluids. Foong *et al.* (2009) conducted a numerical study to investigate the fluid flow and heat transfer characteristics of a microchannel with longitudinal internal fins using water as working fluid. They concluded that internal fins provide heat transfer augmentation and found an optimal fin height that provides the best heat transfer and pressure drop characteristics. Strandberg and Das (2010) developed a trial and error algorithm to determine the performance of a finned-tube heating unit with nanofluids. They found performance increasing when using nanofluids in comparison with a conventional heat transfer fluid. Likewise, Seyf and Feizbakhshi (2012) performed a numerical investigation on the application of nanofluids in Micro-Pin-Fin Heat Sinks. Their results show an effect of the volume fraction and size of the particles on the enhanced heat transfer. On the other hand, a numerical study performed by Lelea and Cioabla (2010) focused on the impact of viscous dissipation on heat transfer in microchannels. They showed that the higher the Brinkman number the longer the thermal entrance will be. Finally a review on heat transfer and fluid flow characteristics in microchannels using nanofluids was presented by Mohammed *et al.* (2011).

In this paper we present a numerical study for convective heat transfer and fluid flow performance of a square microchannel heat sink having internal longitudinal fins using water-based nanofluids as cooling fluids. The fluids considered for this study, containing Al_2O_3, CuO, and ZnO particles respectively, were subjected to a constant heat flux through the walls of the channel. We studied the effect of the type of nanofluid on the heat transfer and pressure drop in the microchannel. In Section II, we present a schematic diagram of the microchannel, describe the model formulation, and the boundary conditions are summarized. In Section III, we discuss the results obtained from simulations. In Section IV, we include concluding remarks.

II. MODEL FORMULATION

The square microchannel with four longitudinal internal fins is shown in Fig. 1(a). Due to the symmetry planes, a quarter of the cross-section of channel is considered in computations, which reduces the number of nodes required and therefore the number of iterations for convergence. The microchannel is 200 μm × 200 μm in cross-section, and 50 mm in length. The whole microchannel, including the internal fins, is considered to be made of aluminum. Table 1 shows the microchannel heat sink dimensions and simulation parameters.

Assuming incompressible laminar steady-state flow, Re < 2300 (Kockmann, 2008), along with appropriated boundary conditions, the continuity, Navier-Stokes, and energy equations were solved using the finite element based software COMSOL Multiphysics®. The full three-dimensional conjugate heat transfer model was used for computations as follow:

Continuity equation:

$$\nabla \cdot (\rho_{eff}\,\mathbf{v}) = 0, , \tag{1}$$

Momentum equation:

$$\rho_{eff}\,(\mathbf{v}\cdot\nabla\mathbf{v}) = -\nabla p + \nabla(\mu_{eff}\nabla\cdot\mathbf{v}), \tag{2}$$

Energy equation:

$$\rho_{eff}\,C_{p,eff}\,(\mathbf{v}\cdot\nabla T) = \nabla\cdot(k_{eff}\nabla T) + \tau:\nabla\mathbf{v}., \tag{3}$$

where the last term on the right-hand side of Eq. 3 represents the viscous dissipation. Considering the nanofluids as Newtonian fluids, the viscous stress tensor is then given by (Deen, 1998):

$$\tau = \mu_{eff}\left[(\nabla\mathbf{v}) + (\nabla\mathbf{v})^T\right], \tag{4}$$

The following boundary conditions, corresponding to Fig. 1(b), were established for the system of partial differential equations:

- Symmetrical boundary condition along dashed lines:

Table 1: Values of the parameters used in the simulations

Parameter	Value
L (mm)	50
H (μm)	180
t_f (μm)	20
t_w (μm)	10
d (μm)	40
q_0" (W/m^2)	5.5×10^5
T_{in} (K)	300
v_{in} (m/s)	5
d_p (nm)	50
ϕ	0.07

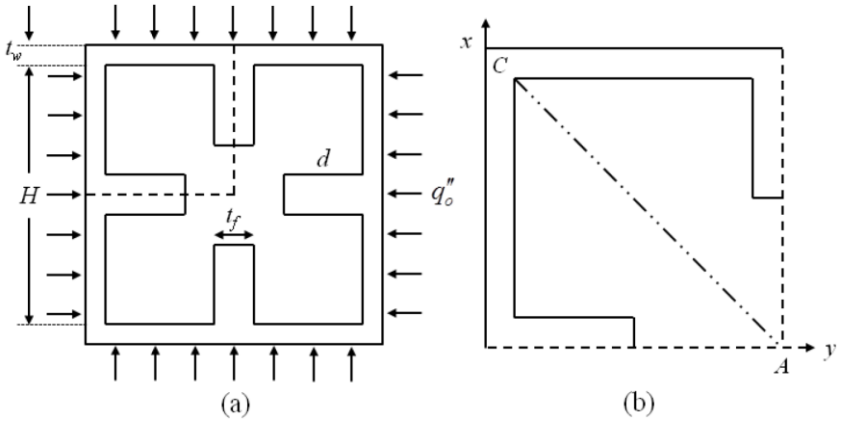

Fig. 1. (a) Schematic diagram of cross section of the microchannel heat sink with internal longitudinal fins. (b) Simulation domain showing the diagonal AC.

$$\mathbf{n}\cdot(k_{eff}\nabla T)=0$$
$$\mathbf{n}\cdot\boldsymbol{\tau}=0$$

- Constant heat flux boundary condition on external surface:

$$\mathbf{n}\cdot(k_w\nabla T)=q_0''$$

- Conjugate heat transfer implies the continuity of temperature and heat flux at the solid-fluid interface, in addition to the non-slip condition.

$$T_w=T_f$$
$$\mathbf{n}\cdot(k_w\nabla T)=\mathbf{n}\cdot(k_{eff}\nabla T)$$
$$\mathbf{v}=0$$

- At the inlet cross-section, z=0, uniform velocity and temperature fields were considered.

$$\mathbf{v}=v_{in}\mathbf{e}_z;\quad T=T_{in}$$
$$\mathbf{n}\cdot(k_{eff}\nabla T)$$
$$\mathbf{v}=0$$

- Finally, at the outlet cross-section, z=L, the following boundary conditions were prescribed:

$$\frac{\partial T}{\partial z}=0;\quad \frac{\partial v_z}{\partial z}=0;\quad v_x=v_y=0;\quad p=0$$

The average local Nusselt number and the heat transfer coefficient were obtained from the results of the simulations once the convergence was achieved. The convective heat transfer and Nusselt number on the inside walls of the channel are defined by:

$$h=\frac{q_i''}{(T_w-T_b)}, \tag{5}$$

$$Nu=\frac{hD_h}{k_{eff}}. \tag{6}$$

In (5) and (6) T_w is the local average wall temperature, and T_b is the local bulk fluid temperature defined as:

$$T_b=\frac{\int_A \rho_{eff}(\mathbf{n}\cdot\mathbf{v})c_{p,eff}TdA}{\int_A \rho_{eff}(\mathbf{n}\cdot\mathbf{v})c_{p,eff}dA}. \tag{7}$$

All thermophysical properties of the nanofluids are considered temperature dependent. The effective viscosity of the water-based Al_2O_3 nanofluid is calculated from the relation given in (Abu-Nada, 2009):

$$\mu_{Al_2O_3}=-0.155-\frac{19.582}{T}+0.794\phi+\frac{2094.47}{T^2}-0.192\phi^2-8.11\frac{\phi}{T}-\frac{27463.863}{T^3}+0.0127\phi^3+1.6044\frac{\phi^2}{T}+2.1754\frac{\phi}{T^2}. \tag{8}$$

Because the lack of experimental data for the ZnO nanofluid, the Brinkman's equation is used to calculate the effective viscosity $\mu_{ZnO}=\mu_{H_2O}(1\text{-}\phi)^{-2.5}$. On the other hand, the viscosity of the CuO nanofluid is correlated as a function of the temperature from the experimental data reported by Nguyen *et al.* (2009).

The effective thermal conductivity of the nanofluids is obtained using the model developed by Vajjha and Das (2010):

$$k_{eff}=\frac{k_p+2k_{bf}-2(k_{bf}-k_p)\phi}{k_p+2k_{bf}+(k_{bf}-k_p)\phi}k_{bf}+\cdot \tag{9}$$

$$+5\times10^4\beta\phi\rho_{bf}c_{p,bf}\sqrt{\frac{\kappa T}{\rho_p dp}}f(T,\phi),$$

where,

$$f(T,\phi)=(2.8217\times10^{-2}\phi+3.917\times10^{-3})\left(\frac{T}{T_0}\right)+(-3.0669\times10^{-2}\phi-3.91123\times10^{-3}),$$

T_0 is the reference temperature, 273 K, and β is a parameter which is in terms of the volume fraction of the particles.

In addition, the effective density and specific heat of the nanofluids are calculated by mixing theory (Smith and Van Ness, 2005):

$$\rho_{eff}=\rho_{bf}(1-\phi)+\rho_p\phi. \tag{10}$$

$$c_{p,eff}=c_{p,bf}(1-\phi)+\rho_{p,p}\phi. \tag{11}$$

III. RESULTS AND DISCUSSION

Following the methodology used by Foong *et al*. (2009), in order to validate the modeling scheme, the unfinned channel results from Lee and Garimella (2006) were compared with an unfinned square channel modeled in the present work. Figure 2 shows the average local Nusselt number for water as a function of the distance from the channel entrance. Clearly, as seen from Fig. 2, the simulation results in the present study agree well with those obtained by Lee and Garimella (2006).

Based on the numerical results, Fig. 3 shows colored temperature contours of one quarter of a cross-sectional area of the microchannel heat sink with water and water-based nanofluids subjected to fixed heat flux of 5.5 × 10^5 W/m^2.

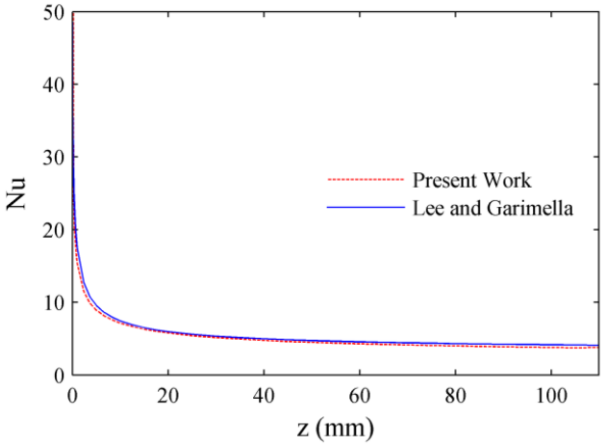

Fig. 2. Comparison of the average local Nusselt number results for an unfinned microchannel with those from Lee and Garimella (2006) for water as coolant.

Figure 3(a) shows that, when water is used as coolant, the center region is cooler than when using nanofluids, indicating a maximum temperature difference around 40ºC between the microchannel walls and the coolant. However, for the case of nanofluids, the CuO nanofluid exhibits higher temperature in the central region than the other ones, as shown in Fig. 3(d), exhibiting additionally a higher temperature on the

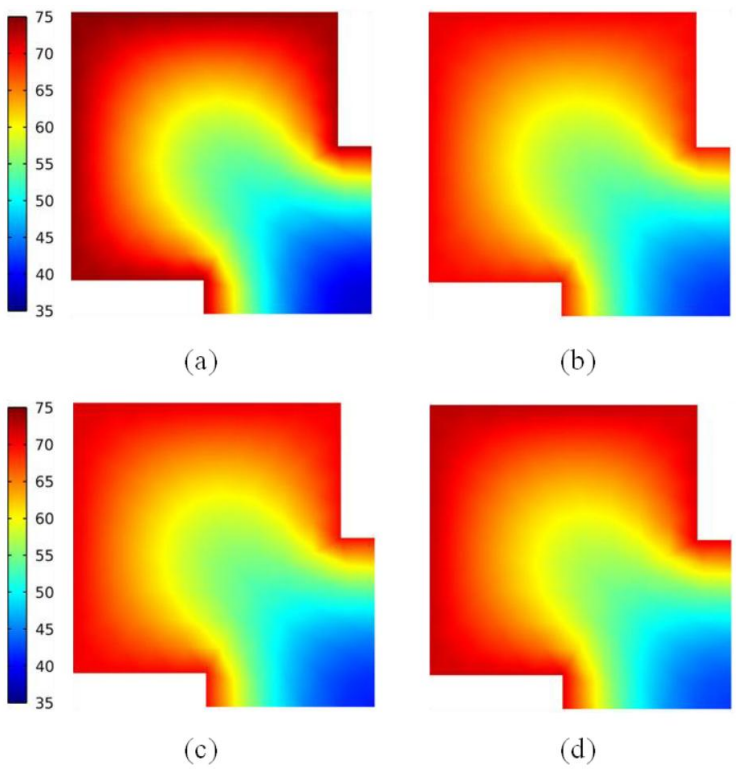

Fig. 3. Temperature contours (ºC) for the different water-based nanofluids at 40 mm from the entrance: (a) H_2O, (b) Al_2O_3, (c) ZnO, and (d) CuO.

walls. Figure 4 shows the temperature variation across the diagonal AC for all the fluids considered in this study. Clearly the CuO nanofluid exhibits the higher temperature along the diagonal, as mentioned above, whereas Al_2O_3 and ZnO nanofluids show no significant differences, as can be seen in Fig. 3(b) and 3(c) as well. On the other hand, the figure shows a steeper slope for water, indicating lower heat transfer rate.

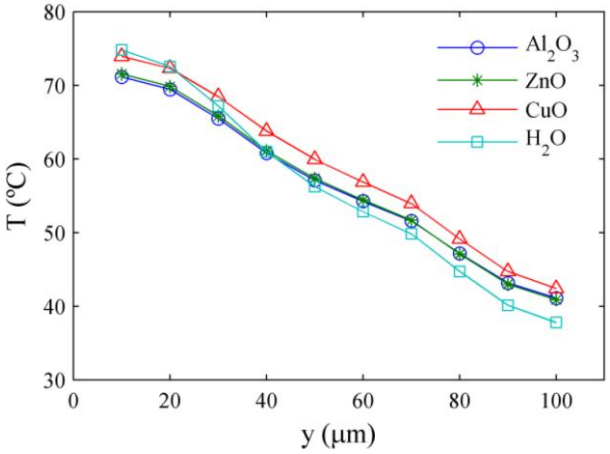

Fig. 4. Temperature distribution along the diagonal AC (see Fig. 1b) at 40 mm from the entrance.

The effect of type of fluid on the average local heat transfer coefficient is shown in Fig. 5 as a function of distance from the inlet of the channel. Larger heat transfer coefficients are observed at the entrance of the channel due to development of the thermal boundary layer. The average heat transfer coefficient decays to a constant value, associated with the fully developed thermal conditions, at the second half of the microchannel. As shown in Fig. 5, nanofluids exhibit higher average heat transfer coefficients than water, showing furthermore that the material of the suspended nanoparticle has no significant effect on the average heat transfer coefficient. Moreover, the results show an increase in the heat transfer, around 40%, when using internal fins in comparison with an unfinned microchannel.

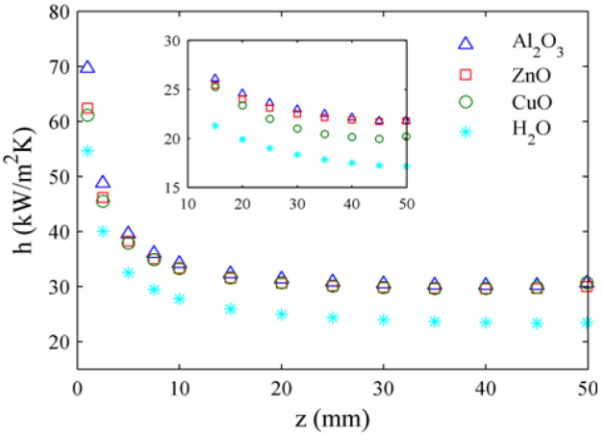

Fig. 5. Average local convective heat transfer coefficient as a function of the microchannel length. Inset, average local convective heat transfer coefficient for an unfinned microchannel.

On the other hand, Fig. 6 shows that the average local Nusselt number converges asymptotically to a fully developed value at the outlet of the channel, which is found to be around 4.0 for all the fluids considered, including nanofluids. However, as observed in Fig. 6 and contrary to the results obtained by Fong *et al*. (2009) for water as coolant, Nusselt number slightly increases

when compared with an unfinned microchannel, which can be attributed to the fact that a larger internal surface area results in a lower internal heat flux (see Eq. 5).

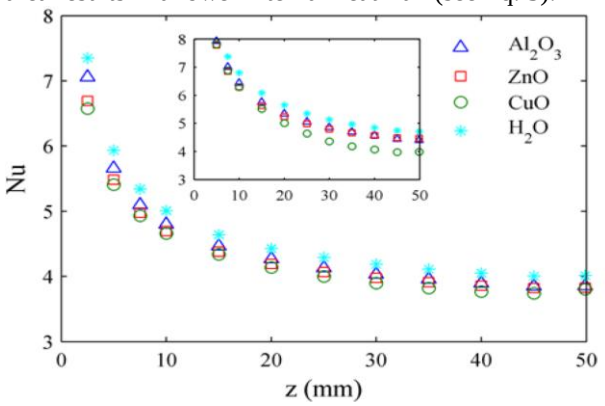

Fig. 6. Average local Nusselt number as a function of the microchannel length. Inset, Nu for an unfinned microchannel.

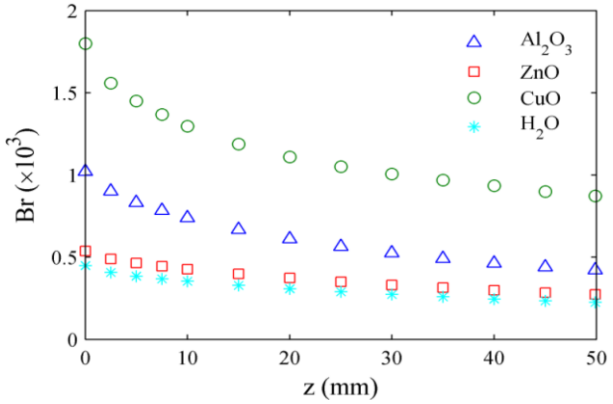

Fig. 7. Variation of the Brinkman number along the microchannel.

On the other hand, Nusselt number is not a good indicator of the increased heat transfer coefficient for nanofluids, since Nu contains the fluid's thermal conductivity (Das *et al*., 2008).

The effect of the viscous dissipation on the heat transfer in the microchannel is analyzed through the Brinkman number, which for constant wall heat flux is defined by (Das *et al.*, 2008):

$$Br = \frac{v_m^2 \mu_{eff}}{q_i'' D_h}. \tag{12}$$

The Brinkman number is plotted in Fig. 7 as a function of the length of the microchannel. Since larger viscosities, nanofluids exhibit Brinkman numbers larger than water, indicating a greater effect of the viscous dissipation on the temperature profile developing. This effect is more significant for the CuO nanofluid since it exhibits the highest viscosity of the fluids considered for the study. Besides the viscosity, the small hydraulic diameter of the microchannel, in addition to the presence of internal fins, leads to high velocity gradients into the flow, thus increasing the effect of the viscous dissipation.

On the other hand, as shown in Fig. 7, the effect of the viscous dissipation decreases to the end of the microchannel, where the viscosity of all fluids considered is lower due to the increasing of the temperature.

The cooling performance of MCHS can be evaluated by the thermal resistance, which is defined as (Jang and Choi, 2006; Mohammed *et al.*, 2010):

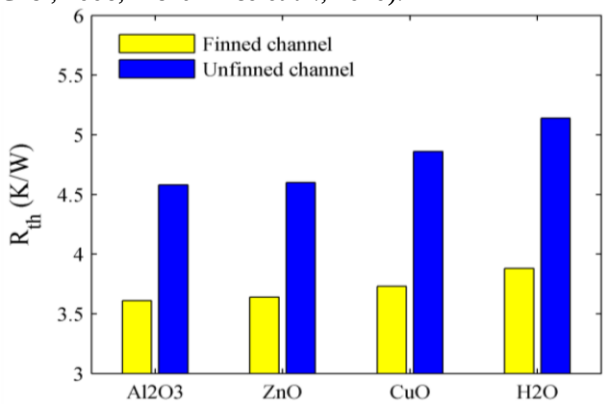

Fig. 8. Thermal resistance of the MCHS for the different water-based nanofluids.

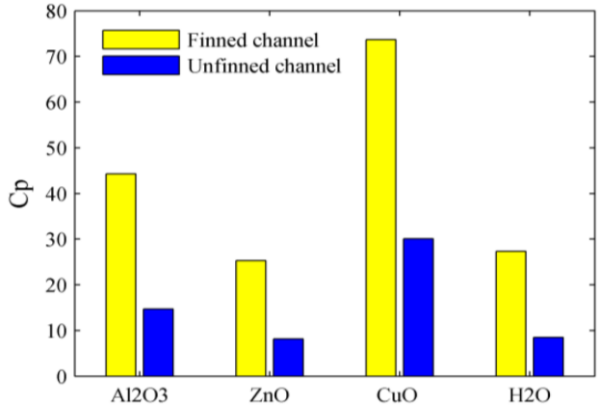

Fig. 9. Pressure coefficient for flow of the different water-based nanofluids trough the microchannel.

$$R_{th} = \frac{T_{w,\max} - T_{in}}{q}. \tag{13}$$

where q is the total heat load applied. Figure 8 shows that nanofluids reduce the thermal resistance since the maximum wall temperature of nanofluid-cooled MCHS is lower than that of water-cooled MCHS. For instance, Figure 3 shows higher wall temperature for water as coolant than nanofluids. Furthermore, finned microchannel exhibits lower thermal resistance which is attributed to the presence of fins that result in higher heat transfer rate and therefore lower wall temperature.

Other important parameter to take into account for flow through a microchannel is the pressure drop. Thus, the dimensionless pressure drop, known as the pressure coefficient, is shown in Fig. 9 for the different fluids considered. The pressure coefficient is calculated as:

$$Cp = \frac{\Delta p}{\frac{1}{2}\rho v_{in}^2}. \tag{14}$$

From Fig. 9, it can be seen that Al_2O_3 and CuO nanofluids exhibit larger pressure drop, whereas no significant difference exist between pure water and ZnO nanofluid, which may be caused by the viscosity presumption made for ZnO nanofluid through the Brinkman's equation. Thus, further studies, showing the effect of using different viscosity equations on the pres-

sure drop calculations, are necessary to show if any advantage of use ZnO nanofluid as coolant in microchannel heat sinks. The reason of higher pressure drop for nanofluids is due to the fact that the presence of particles increases the viscosity of the suspension for force- and torque-free suspended particles, as first estimated by Einstein (1906, 1911) for a suspension of rigid spherical particles. This fact, combined with larger wall surface area, due to the presence of internal fins, leads to high values of the pressure drop through the microchannel compared with the unfinned one.

IV. CONCLUSIONS

Using numerical simulations we have studied the effect of internal fins and nanofluids, as coolant fluids, in MCHS subjected to constant heat flux. The governing mass, momentum, and energy equations were solved numerically together with appropriate boundary conditions using COMSOL Multiphysics®. The variation of the convective heat transfer coefficient along the microchannel as well as the pressure drop was determined. Three different water-based nanofluids were simulated: Al_2O_3, CuO, and ZnO.

Simulations results show a considerable effect of using nanofluids as coolant fluids in microchannel heat sinks with internal longitudinal fins. High convective heat transfer coefficients and pressure drop were found for the fluids studied. This fact is attributed to the presence of internal fins. On the other hand, nanofluids show higher convective heat transfer and pressure drop in the MCHS relative to water. This enhancement is due to the presence of suspended nanoparticles as they change the physical properties of the base fluid. It was showed also that Nu is not a good parameter to compare the heat transfer enhancement of nanofluids. Viscous dissipation exhibits a significant effect on the heat transfer in the MCHS as observed through the Brinkman number, which increases to the entrance of the microchannel. Finally, the thermal resistance of MCHS decreases when using nanofluids as coolant fluids.

ACKNOWLEDGEMENTS

The authors acknowledge the financial support of the Department of Chemical Engineering, Universidad Pontificia Bolivariana.

NOMENCLATURE

Br	Brinkman number
c_p	specifc heat, J/kg K
C_p	pressure coefficient
d	fin height, nm
d_p	particle's diameter, nm
D_h	hydraulic diameter, m
e	unit vector
h	heat transfer coefficient, W/m^{2}K
H	height of the channel, nm
k	thermal conductivity, W/mK
L	microchannel length, mm
n	normal unit vector
Nu	Nusselt number
p	pressure, N/ m^2
q	heat transfer rate, W
q''	heat flux, W/ m^2
R_{th}	thermal resistance, K/W
T	temperature, K
t_w	wall thickness, nm
t_f	fin thickness, nm
v	velocity vector, m/s
v	velocity component, m/s
x, y, z	spatial coordinates

Greek symbols

ϕ	particle's volume fraction
μ	viscosity, Pa s
ρ	density, kg/m^3
κ	Boltzmann constant, Jouls/s
∇	del operator
τ	viscous stress tensor, N/m^2

Subscripts

b	bulk
bf	base fluid
eff	effective
f	fluid
in	inlet
i	inside
m	average
o	outside
p	particle
w	wall

Superscripts

T	transpose

REFERENCES

Abu-Nada, E., "Effects of variable viscosity and thermal conductivity of Al2O3-water nanofluid on heat transfer enhancement in natural convection," *Int. J. Heat Fluid Flow*, **30**, 679-690 (2009).

Bhattacharya, P., S.K. Saha, A. Yadav, P.E.. Phelan and R.S. Prasher, "Brownian dynamics simulation to determine the effective thermal conductivity of nanofluids," *J. Appl. Phys*., **95**, 6492-6494 (2004).

Chein, R. and G. Huang, "Analysis of microchannel heat sink performance using nanofluids," *Appl. Therm. Eng.*, **25**, 3104-3114 (2005).

Chein, R. and J. Chuang, "Experimental microchannel heat sink performance studies using nanofluids," *Int. J. Therm. Sci.*, **46**, 57-66 (2007).

Choi, S.U.S. and J.A. Eastman, "Enhancing thermal conductivity of fluids with nanoparticles," *Mater. Sci.*, **231**, 99-105 (1995).

Das, S.K., S.U.S. Choi, W. Yu and T. Pradeep, *Nanofluids: Science and technology*, John Wiley & Sons, New Jersey (2008).

Deen, W.M. *Analysis of transport phenomena*, Oxford University Press, New York, (1998).

Einstein, A., "Eine neue bestimmung der molekuldimensionen," *Annalen der Physik*, **324**, 289-306 (1906).

Einstein, A., "Berichtigung zu meiner arbeit: "Eine neue bestimmung der molekuldimensionen"," *Annalen*

der Physik, **339**, 591-592 (1911).

Foong, A.J.L., N. Ramesh and T.T. Chandratilleke, "Laminar convective heat transfer in a microchannel with internal longitudinal fins," *Int. J. Therm. Sci.*, **48**, 1908-1913 (2009).

Godson, L., B. Raja, D. Mohan Lal and S. Wongwises, "Enhancement of heat transfer using nanofluids—An overview," *Renewable Sustainable Energy Rev.*, **14**, 629-641 (2010).

Heris, S.Z., S.G. Etemad and M.N. Esfahany, "Experimental investigation of oxide nanofluids laminar flow convective heat transfer," *Int. Commun. Heat Mass Transfer*, **33**, 529-535 (2006).

Ijam, A. and R. Saidur, "Nanofluid as a coolant for electronic devices (cooling of electronic devices)," *Appl. Therm. Eng.*, **32**, 76-82 (2012).

Jang, S.P. and S.U.S. Choi, "Role of Brownian motion in the enhanced thermal conductivity of nanofluids," *Appl. Phys. Lett.*, **84**, 4316-4318 (2004).

Jang, S.P. and S.U.S. Choi, "Cooling performance of a microchannel heat sink with nanofluids," *Appl. Therm. Eng.*, **26**, 2457-2463 (2006).

Jung, J.Y., H.-S. Oh and H.-Y. Kwak, "Forced convective heat transfer of nanofluids in microchannels," *Int. J. Heat Mass Transfer*, **52**, 466-472 (2009).

Kakac, S. and A. Pramuanjaroenkij, "Review of convective heat transfer enhancement with nanofluids," *Int. J. Heat Mass Transfer*, **52**, 3187-3196 (2009).

Keblinski, P., S.R. Phillpot, S.U.S. Choi and J.A. Eastman, "Mechanism of heat flow in suspensions of nano-sized particles (nanofluids)," *Int. J. Heat Mass Transfer*, **45**, 855-863 (2002).

Kockmann, N. *Transport phenomena in micro process engineering*, Springer, Berlin, (2008).

Lee, P.S. and S.V. Garimella, "Thermally developing flow and heat transfer in rectangular microchannels of different aspect ratios," *Int. J. Heat Mass Transfer*, **49**, 3060-3067 (2006).

Lelea, D., "The performance evaluation of Al2O3/water nanofluid flow and heat transfer in microchannel heat sink," *Int. J. Heat Mass Transfer*, **54**, 3891-3899 (2011).

Lelea, D. and A.E. Cioabla, "The viscous dissipation effect on heat transfer and fluid flow in micro-tubes," *Int. Commun. Heat Mass Transfer*, **37**, 1208-1214 (2010).

Mohammed, H.A., G. Bhaskarana, N.H. Shuaiba and R. Saidurb, "Heat transfer and fluid flow characteristics in microchannels heat exchanger using nanofluids: A review," *Renewable Sustainable Energy Rev.*, **15**, 1502-1512 (2011).

Mohammed, H.A., P. Gunnasegaran and N.H. Shuaib, "Heat transfer in rectangular microchannels heat sink using nanofluids," *Int. Commun. Heat Mass Transfer*, **37**, 1496-1503 (2010).

Nguyen, C.T., F. Desgranges, G. Roy, N. Galanis, T. Maré, S. Boucher, H. Angue Mintsa, "Temperature and particle-size dependent viscosity data for water-based nanofluids - Hysteresis phenomenon," *Int. J. Heat Fluid Flow*, **28**, 1492-1506 (2007).

Prasher, R., P. Bhattacharya and P.E. Phelan, "Thermal conductivity of nanoscale colloidal solutions (nanofluids)," *Phys. Rev. Lett.*, **94**, 025901 (2005).

Prasher, R., P. Bhattacharya and P.E. Phelan, "Brownian motion based convective-conductive model for the effective thermal conductivity of nanofluids," *J. Heat Transfer*, **128**, 588-595 (2006).

Seyf, H.R. and M. Feizbakhshi, "Computational analysis of nanofluid effects on convective heat transfer enhancement of micro-pin-fin heat sinks," *Int. J. Therm. Sci.*, **58**, 168-179 (2012).

Smith, J.M. and H. Van Ness, *Introduction to chemical engineering thermodynamics*, McGraw-Hill, New York (2005).

Sobhan, C.B. and G.P. Peterson, *Microscale and nanoscale heat transfer: Fundamentals and engineering applications*, CRC Press, Boca Raton (2008).

Strandberg, R. and D.K. Das, "Finned tube performance evaluation with nanofluids and conventional heat transfer fluids," *Int. J. Therm. Sci*, **49**, 580-588 (2010).

Tuckerman, D.B. and R.F. Pease, "High performance heat sinking for VLSI," *IEEE Electron Device Lett.*, **EDL-2**, 126-129 (1981).

Vajjha, R.S. and D.K. Das, *Measurements of nanofluids properties and heat transfer computation*, LAP LAMBERT Academic publishing, Saarbrücken, (2010).

Received: July 19, 2012
Accepted: October 7, 2012
Recommended by Subject Editor: Walter Ambrosini